High sensitivity measurements of gas transport through films for food packaging and the O₂ adsorption issue

Marine Schott [a], Janez Setina [b], Espedito Vassallo [c], Matteo Pedroni [c], Roberta Campardelli [d], Patrizia Perego [d], Luca Repetto [a], Giuseppe Firpo [a,*]

[a] Department of Physics, University of Genoa, Via Dodecaneso 33, 16146, Genova, Italy
[b] Institute of Metals and Technology (IMT), Lepi Pot 11, Ljubljana, SI, 1000, Slovenia
[c] Institute for Plasma Science and Technology (ISTP), National Research Council-CNR, Via R. Cozzi 53, Milan, 20125, Italy
[d] Department of Civil, Chemical and Environmental Engineering, University of Genoa, Via Opera Pia, 15, 16145, Genoa, Italy

ABSTRACT

New biodegradable polymers employed for food packaging require an accurate characterization of their O_2 ultra-barrier permeation rates. Methods and procedures of gas transport measurements must guarantee high sensitivity and immunity to artefacts. Within this context, this paper reports two outcomes. The first one is to demonstrate the suitability of a specific high vacuum apparatus for challenging measurements of gas permeability on new polymers for food packaging. We show that our newly developed set-up is able to achieve a minimum detectable gas throughput $2 \times 10^{-9} mbar\, l / s$, which is equivalent to permeability coefficient of $7 \times 10^{-11}\ cm^2/s$ in case of 20 μm-thick polymer film with an area of $7 \times 10^{-2}\ cm^2$ under a $10^5\ Pa$ pressure differential. The second aim is to investigate the origin of its detection limits and possible measurement artefacts obtained with this instrument. In particular, we focus on the O_2 adsorption effect on the inner surfaces of the set-up.

1. Introduction

The selection of materials used for food packaging has recently been expanded to include films with tailored properties such as an antioxidant activity and biodegradability [1]. These materials are always chosen to maintain a strong barrier to oxygen to keep a long shelf-life of the products. A proper characterization of the efficiency of this barrier is obtained by quantifying the oxygen gas transmission rate (O₂GTR), defined as the quantity of oxygen passing through a unit area of the parallel surfaces of a plastic film per unit time under the test conditions. The American Society for Testing and Materials International (ASTM) Designation F 2622–08 recommends that conditions of test, including temperature and oxygen partial pressure on both sides of the film, must be stated [2]. In this work we use the permeability coefficient P to characterize materials as defined in Ref. [2]. In general, the choice of experimental methods and procedures to measure O₂GTR, as well as P for O_2 and other gases, requires care, as recommended in ASTM Designation. In the case of strong oxygen-barrier films, a special attention must be taken because of the extremely low permeability of these materials. The most used packaging materials have oxygen permeability

coefficient P in the range $(10^{-9} \div 10^{-13})\ cm^2/s$ [3]. Consequently, techniques to characterize them with respect to the gas they are protecting from, must provide high sensitivity and must be free even of artefacts that are usually considered as negligibly impacting.

State of the art technology employs different techniques for polymer characterization [4]: the isostatic [5] and the manometric [6] being the most used methods. Several companies provide products operating with these technologies, but manufacturers of instruments based on the isostatic method using coulometric sensors [7] claim advantage over manometric-based technology in terms of accuracy, repeatability, and ease of use. However, instrumentations with coulometric or optical detectors [8] are available only for one specific tracer gases, mainly O_2, CO_2, and water vapor (WV). Moreover, equipping manometric set-ups with mass spectrometers has helped to develop measurement instruments with extremely high accuracy and a better versatility with respect to coulometric based technology [9–11]. Zhang et al. [11] demonstrate an accumulation technique for permeation measurements, including reactive and condensable gases. This technique meets sensitivity requirements for O_2 ultra-barrier and for WV permeation rates for organic light emitting diodes (OLEDs) flexible display. As a
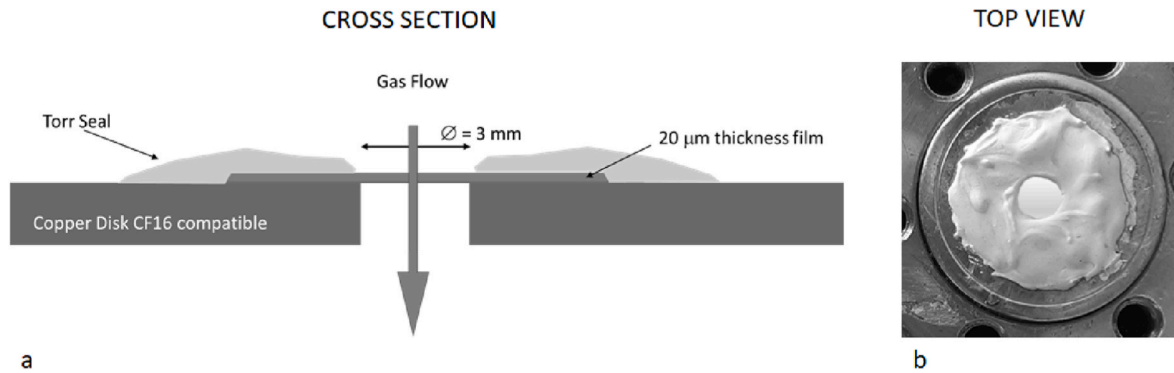
Fig. 1. Sample's Assembly for PLA, BL, BLc. (a) Cross section with dimensions (b) image of the copper disk top view.

consequence, this technique is, in principle, also suitable to the range of permeabilities aimed for gas-barrier film in the context of food packaging application. They also report a detection limit for WV, nitrogen and carbon dioxide that is two orders of magnitude lower than the corresponding values offered by the NIST-traceable standard techniques. Besides, the authors notice some particularities in oxygen detection, but they do not consider the effect of O_2 surface adsorption on the inner walls of the vacuum chamber.

The first purpose of this work is to extend the applicability of the high vacuum set-up described by Firpo et al. [10] where the authors report the measurement of a permeability coefficient of $(6.2 \pm 0.6) \times 10^{-8} \ cm^2/s$, obtained for He through Viton®. More precisely, we show O_2 permeability measurements through polyethylene terephthalate (PET) and O_2 and CO_2 permeabilities through other pristine and coated biodegradable polymers recently suggested as packaging materials, the coating being deposited to significantly enhance the barrier protection against oxygen [12].

The second purpose of the present paper is to identify the limiting factors for the sensitivity of the aforementioned apparatus and to discuss possible artefacts affecting the measurements. In particular, we will focus on O_2 permeation measurements, extending the analysis of ref. [11], where the authors declare, for their apparatus, a detection limit for O_2 permeation higher than the offered by the standard techniques. They consider the chemical reactions of O_2 on or near the hot filament of the residual gas analyser (RGA) as a potential cause of this limit in sensitivity in O_2 partial pressure measurement. This work is going a step further, considering also the adsorption of O_2 and other gases on the inner walls of the vacuum chamber. The relevance of the phenomenon has been already pointed out in Ref. [13], where the evidence that oxygen undergoes an efficient adsorption on vacuum degassed stainless steel 304 at $20°C$ is reported. To this purpose, we report for the same samples, gas transport measurements with CO_2 and N_2. By comparing the results for CO_2 and N_2 with those for O_2 we could confirm the previous hypothesis.

2. Materials and methods

2.1. Experimental set-up

Permeation measurements are carried out with the set-up described in Ref. [10]. This apparatus operates with two different methods that we identify as dynamic and static. Both these methods are employed to deduce the permeability coefficient P of the polymers. The dynamic method relies on the use of a RGA, while the static one uses a spinning rotor gauge (SRG) and the system can be calibrated in-situ. The sample assembly has been designed and implemented to guarantee an identical exposed area for the upstream and the downstream sides, thus avoiding errors on the calculations necessary to obtain P.

2.2. Samples

The biodegradable polymers tested with O_2 and CO_2 (typical test gases for film for food packaging) are polylactic acid (PLA) and a blend (BL) of polybutylene adipate terephthalate (PBAT)/PLA with 60% and 40% in weight respectively. We also measure permeability coefficient to O_2 for a PET sample. Further measurements are carried out with O_2, CO_2 and N_2 for the biodegradable polymer BL with a 25 nm coating of SiO_x (BLc). N_2 is used for a direct comparison with a non-reactive gas, expecting it not to be sensible to potential phenomenon induced by reactivity inside the chamber. The BL coating is deposited by plasma enhanced chemical vapor deposition (PECVD).

All samples, except PET, are 20 μm-thick films, provided by Corapack S. r.l. Italy. PET is 100 μm-thick films provided by Sigma-Aldrich, now Merck KGaA Germany. The samples are glued on a 3 mm-circular hole (for PET 5.5 mm-circular hole), drilled in a copper disk compatible with a ConFlat (CF) flange 16, by means of Torr Seal® sealant, as shown in Fig. 1 for PLA, BL and BLc samples.

The sealant is deposited in such a way that the total area exposed to the gas flow is preserved and equal to 7 mm² (for PET area is 24 mm²). Small deviations in the geometry are quantified by direct imaging technique. The size of the area is chosen as a trade-off between the requirement to maintain a high flux (high sensitivity) and to ensure mechanical integrity for the polymeric film under a $10^5 \ Pa$ pressure differential. As reported in Ref. [10], this assembly ensures vacuum sealing with negligible leak losses during experiments.

2.3. Procedures

The permeability coefficient, as defined in Ref. [14], which is the same definition in Ref. [2] extend to any gases, is obtained by the formula

$$P = \frac{JL}{\Delta p}, \tag{1}$$

where J is the gas transmission rate in $molm^{-2}s^{-1}$, L is the sample thickness in m and $\Delta p = p_u - p_d$ is the differential pressure across the sample with p_u and p_d upstream and downstream pressure in Pa, respectively. In the dynamic method J is calculated by means of RGA measurements of the partial pressure p_d of the tracer gas, by the formula

$$J = \frac{p_d s}{A}, \tag{2}$$

where s is the effective pumping speed and A is the area of the sample in m^2. The RGA is re-calibrated before each round of measurements. In the static procedure the system is considered as a constant-volume/variable-pressure apparatus, the gas transmission rate is given by the formula

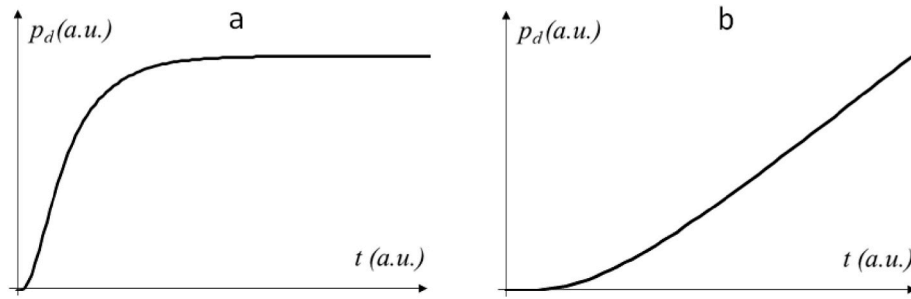$$J = \frac{V}{A} \frac{\partial p_d}{\partial t}, \tag{3}$$

Fig. 2. Theoretical trend for downstream pressure expression according to the diffusion model: a) for dynamic method, b) for static method.

where V is the chamber volume in m^3 and $\partial p_d/\partial t$ is estimated by the slope of the raise of pressure in steady state. In this case the pressure is measured by the SRG.

All measurements are carried out with an upstream pressure of tracer gas of $10^5\ Pa$ that, considering downstream pressure range is between $10^{-6}\ Pa$ and $1\ Pa$ result in a differential pressure $\Delta p = 10^5\ Pa$ across the film. To guarantee the same conditions for the inner surfaces of the vacuum chamber for every set of measurements, the system is always pumped and baked with the procedure described in Ref. [10]. Further details on the instrumentation, its calibrations and its accuracy can be found in Ref. [10].

2.4. Sample conditioning

A potential concern involves the pre-adsorbed environmental moisture inside the material, typical of polymer samples, which can lead to unreliable results. In our measurements, the sample is maintained in vacuum for several hours and experiences a bakeout before the tests. These measurements techniques and conditions help to reduce considerably moisture degassing. Anyway, if some spurious gas is still present during measurements, it is expected to impact results only for static method for which gas distinction cannot be made. Whereas, when measurements are performed with the dynamic one, the procedure reports a gas-specific partial pressure analysis that is unaffected by a potential moisture degas.

3. Theory

The basic theory of the gas transfer process through dense polymers is well described by the Fick's and Henry's laws and is usually reported as solution-diffusion model (in the following we will call it diffusion model) [15]. Under the hypothesis of near-equilibrium at surfaces, P can be expressed by the formula

$$P = DS, \tag{4}$$

where D is the diffusion coefficient, taken as constant (independent of gas concentration), in $cm^2 s^{-1}$ and S is the dimensionless solubility.

Considering that in our set-up, the film is initially at zero concentration and downstream concentration is maintained at zero, the solution for the total amount of diffusing gas Q_t in $mol\ m^{-2}$ which has passed through the membrane in time t is [eq. 4.24a of Ref. [16]]:

$$\frac{Q_t}{LC_1} = \frac{Dt}{L^2} - \frac{1}{6} - \frac{2}{\pi^2}\sum_1^\infty \frac{(-1)^n}{n^2}exp\left(-\frac{Dn^2\pi^2 t}{L^2}\right), \tag{5}$$

where C_1 is the gas concentration in the upstream side of the membrane.

This could be expressed in dynamic method by:

$$Q_t = \int_0^t J(t)dt = \frac{s}{A}\int_0^t p_d(t)dt, \tag{6}$$

Substituting eq. (6) in (5) and considering eq. (4), we obtain the

Table 1

Permeability coefficient P of O_2 through PET in dynamic method and of CO_2 and O_2 through PLA and BL in dynamic and static method. Values were extracted from measurements using, for PLA and BL, the procedure mentioned in section 2.3, while for PET the one in section 4.1.

Gas	PET	PLA		BL	
	Dynamic	Dynamic	Static	Dynamic	Static
	$P^a(cm^2\ /s)$ $\times 10^{10}$	$P^a(cm^2\ /s)$ $\times 10^9$	$P^a(cm^2\ /s)$ $\times 10^9$	$P^a(cm^2\ /s)$ $\times 10^9$	$P^a(cm^2\ /s)$ $\times 10^9$
O_2	1.3 ± 0.2	2.2 ± 0.3	2.5 ± 0.2	1.5 ± 0.2	1.4 ± 0.1
CO_2		17 ± 3	17 ± 2	15 ± 2	14 ± 1

$^a 1\dfrac{cm^2}{s} = 1\ cm^3(STP)\ cm\ s^{-1}cm^{-2}atm^{-1} = 4.4\times 10^{-8}mol\ m\ m^{-2}\ s^{-1}\ Pa^{-1}$ (at $0°C$)

following expression for the downstream pressure, corrected from its background:

$$p_d(t) = \frac{A\Delta pP}{Ls}\left[1 + 2\sum_1^\infty (-1)^n exp\left(-\frac{Dn^2\pi^2 t}{L^2}\right)\right] \tag{7}$$

In static method we then get:

$$Q_t = \frac{1}{A}\int_0^t \frac{d(pV)}{dt}dt = \frac{V}{A}(p_d(t) - p_d(0)) \tag{8}$$

In this case, substituting eq. (8) in (5) and considering eq. (4), we obtain the following expression for the downstream pressure, corrected from its background:

$$p_d(t) = \frac{AL\Delta pP}{DV}\left[\frac{Dt}{L^2} - \frac{2}{\pi^2}\sum_1^\infty \frac{(-1)^n}{n^2}exp\left(-\frac{Dn^2\pi^2 t}{L^2}\right)\right] \tag{9}$$

Equations (7) and (9) are the respective expressions of the diffusion model for the time evolution of the downstream pressure for dynamic and static methods. The theoretical trend is reported in Fig. 2.

At steady state ($t\to\infty$), eq. (7) gives P in dynamic method with J as in (2), while eq. (9) gives P in static method with J as in (3).

From this theory it is possible to obtain also D by the lag time procedure [16]. In dynamic method D can be obtained by eq. (3) of ref. [10] and in static method with eq. (5) of the same previous references.

4. Results and discussion

Table 1 reports the values of P of two gases of reference O_2 and CO_2 through PET, PLA and BL obtained with our set-up. Data on P of these gases through PET and PLA can be compared directly with performance reported in existing literature. The results show a range of permeability coefficient ranging from $10^{-8}\ cm^2/s$ (CO_2 through PLA) to $10^{-10}\ cm^2/s$ (O_2 through PET). The data of PLA and BL obtained with both methods are consistent within measurement uncertainty. The ratio between their deduced permeability and the mean free path of the gas happened to be
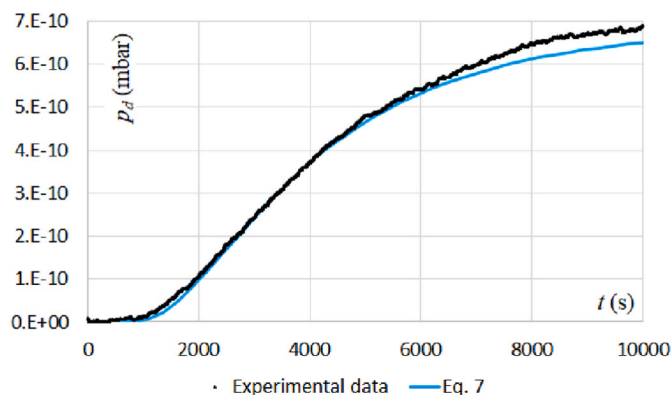
Fig. 3. O_2 **flow through PET.** The graph shows the downstream O_2 partial pressure after filling, at $t = 0$, the upstream chamber with pure O_2 at $10^5\ Pa$. Fitting with diffusion equation is shown in light blue.

varying with gas type, we could notice that this is in contradiction to what is expected for porous media [17,18]. This extra check helped us to assert that we are dealing with dense structure of bio polymers and that we are in the range of applicability of solution-diffusion model.

The result of permeability coefficient of O_2 through PET is obtained only with the dynamic method (see first line of Table 1) as the result obtained with the static method has been ruled out because the downstream pressure measured by SRG does not follow the trend expected from the diffusion equation (eq. (9)). As already discussed in section 2.3, the moisture degas effect during measurements of material with low permeability, affects the downstream pressure values in static method, especially at the start of the measurement.

For PLA and PET, we can notice that O_2 permeability coefficient through PLA is $2.2 \times 10^{-9}\ cm^2/s$ that agrees well with $2.0 \times 10^{-9}\ cm^2/s$ reported in Ref. [19], whereas O_2 permeability coefficient through PET (for which this coefficient tends to be lower than the one of PLA) happens to be lower than the range found in literature going from $3.8 \times 10^{-10}\ cm^2/s$ [20] to $5 \times 10^{-10}\ cm^2/s$ [21]. Differences can be ascribed to well-known phenomena such as different fabrication protocols, polymer aging and plasticization. A possible influence of O_2 surface adsorption on the inner walls of the chamber will discussed in the next section.

The results of O_2-transport measurements through BLc are not reported in Table 1 because of artefacts that will be described in section 4.2. For this material a larger selection of gases has been tested (O_2, CO_2, and N_2) and a refined analysis has been necessary because its permeability coefficient is even lower than the ones for standard PET and PLA.

4.1. PET

As mentioned previously, O_2 measurements through PET are reported only for the dynamic method and the results are presented in Fig. 3.

A fit of the experimental data using the diffusion equation is possible only for the first part of the acquisition. The observed deviation from the expected trend at long times, with the pressure showing a drift instead of reaching a steady value, has been characterized quantitatively in order to establish the subset of the data that can be considered conformal to the diffusion model and thus can be properly used to extract values for P and D. This has been done by repeating, for different truncations of the datasets, the fitting procedure with the model (eq. (7)). For every fit we calculated the coefficient of determination R^2 and considered it as an estimator of the conformity of the dataset with the model. At $t = 6000\ s$, R^2 started to decrease and we considered it as a sign of deviation from the expected trend. Even if the value of P happens to be lower of that report in Ref. [20], the diffusion coefficient D obtained by the fit results to be $3.5 \times 10^{-9}\ cm^2/s$ in agreement with reference [20].

We speculate that the oxygen undergoes an efficient adsorption on the walls of the vacuum chamber as reported in Ref. [13]. In this case, the inner walls of the chamber would act as a "capture pump", for which the pumping speed would decrease when O_2 surface coverage increases. This explanation is compatible with the ongoing increase for the downstream pressure in Fig. 3 and could be the reason of the disagreement of the result with literature. However, because RGA is similar to those used in Ref. [11], we can't exclude other phenomena as O_2 reacting on or near a hot filament of the detector.

4.2. Gas permeation test on BLc: instrument sensitivity and O_2 adsorption effect

To examine the validity of the oxygen adsorption hypothesis we proceed with three different tests of gas transport measurements through coated polymer BLc that we indicate as: dynamic, static long-term and static short-term.

4.2.1. Dynamic test

The test is performed with the dynamic method and on a selection of common gases O_2, CO_2 and N_2. Gas flows through BLc are recorded for a time scale of hundreds of seconds ($t < 500\ s$). The results can be seen on Fig. 4, where the fits of the experimental data for the three gases have been done with the same procedure reported in sec. 4.1 for PET.

Fig. 4 a report the downstream pressure of oxygen and the fit of the experimental data with a solution of the diffusion equation reported in light blue. From the parameters used for the of fit it is possible to obtain a value of gas throughput $2.5 \pm 0.5 \times 10^{-9}\ mbar\ l\ /\ s$. Considering the area and the thickness of the BLc, and experimental conditions of $10^5\ Pa$ of pressure differential across the film, this value correspond to a permeability coefficient $P = 7 \pm 1 \times 10^{-11}\ cm^2/s$. These values show that set-up can achieve, at least, a minimum detectable gas throughput in the range $10^{-9}\ mbar\ l\ /\ s$ and is a proof of our apparatus high sensitivity. However, as already seen for O_2 through PET in Fig. 3, the fit is
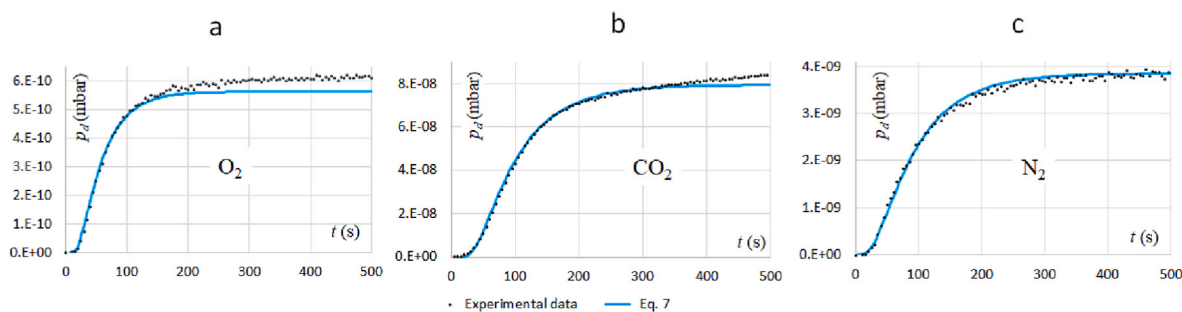
Fig. 4. Downstream pressure of tracer gases through BLc. a) Downstream pressure of O_2, b) Downstream pressure of CO_2 and c) Downstream pressure of N_2 after filling, at $t = 0\ s$, the upstream chamber with, respectively O_2, CO_2 and N_2 (e.g., moving from a pressure p_u of 1 Pa to $10^5 Pa$). Fitting with diffusion equation is shown in light blue.
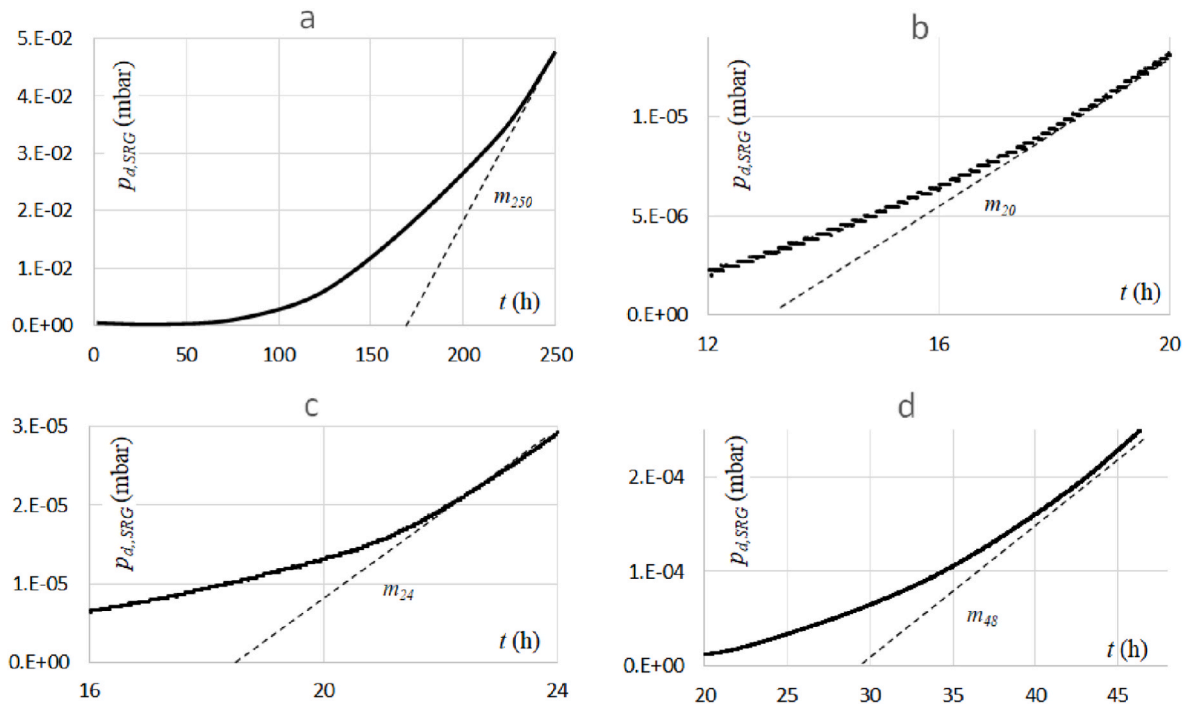
Fig. 5. O_2 **flow through BLc.** Downstream pressure $p_{d,SRG}$ measured by static method. The graphs report the data: a) for the entire ten days of measurements and the slope taken at 250 *hours* ($m_{250} \approx 2 \times 10^{-7}$ *mbar/s*), b) between 12 and 20 *hours* with the slope taken at 20 *hours* ($m_{20} \approx 5 \times 10^{-10}$ *mbar/s*), c) between 16 and 24 *hours* with the slope taken at 24 *hours* ($m_{24} \approx 1 \times 10^{-9}$ *mbar/s*), d) between 20 and 48 h with the slope taken at 48 h ($m_{48} \approx 4 \times 10^{-9}$ *mbar/s*).

reliable only for the first part of the acquisition. After 170 s R^2 started to decrease and we considered it as a sign of deviation from the expected trend. Fig. 4 b and c report downstream pressure of CO_2 and N_2. We observe deviation from the diffusion model after 350 s (R^2 started to decrease) for measurement involving CO_2, while, for N_2, R^2 did not show a significant deterioration for the whole acquisition from 0 s to 500 s. This point indicates that the phenomenon could be peculiar for O_2. From the parameters of the fits it is possible to obtain the diffusion coefficients $D(O_2) = 1.0 \times 10^{-8}$ cm^2/s, $D(CO_2) = 6.0 \times 10^{-9} cm^2/s$ and $D(N_2) = 5.8 \times 10^{-9}$ cm^2/s.

Then, these results are compatible with the O_2 adsorption hypothesis. Consequently, this phenomenon could be another limiting factor for the sensitivity of O_2 permeation measurements, in addition to the degas of the chamber walls at base pressure (Ref. [10]). However, the dynamic method uses an RGA detector that is based on a residual gas ionization by the electrons emitted from a hot filament as the one used by Zhang et al. [11]. For this reason, as in the case of O_2 through PET, to exclude effects of potential chemical reaction of O_2 on or near hot filament, we must complete other tests with a different detector for downstream pressure.

4.2.2. Static long-term test

This test is performed in static method with O_2 and can't be affected by artefact reported in Ref. [11] and in previous section, because the pressure gauge is a SRG, free from hot filaments. Because of the extremely low permeability coefficient of this material, the measurement took 250 *h* to be completed The results of this test are reported in Fig. 5 where we can see the downstream pressure indicated with $p_{d,SRG}$.

The data are not compatible with the diffusion equation (see Fig. 2 b). This can be directly inferred from the trend of $p_{d,SRG}$ *vs* t in the plots covering the full 250 *hours* acquisition where no single slope can be found. Examples of these slopes indicated with m and deduced by linear fit, are: $m_{250} \simeq 2 \times 10^{-7}$ *mbar/s* (Fig. 5 (a)), $m_{20} \simeq 5 \times 10^{-10}$ *mbar/s* (Fig. 5 (b)), $m_{24} \approx 1 \times 10^{-9}$ *mbar/s* (Fig. 5 (c)), and become $m_{48} \approx 4 \times 10^{-9}$ *mbar/s* (Fig. 5 (d)) at 48 *hours*. This variation of slope can be
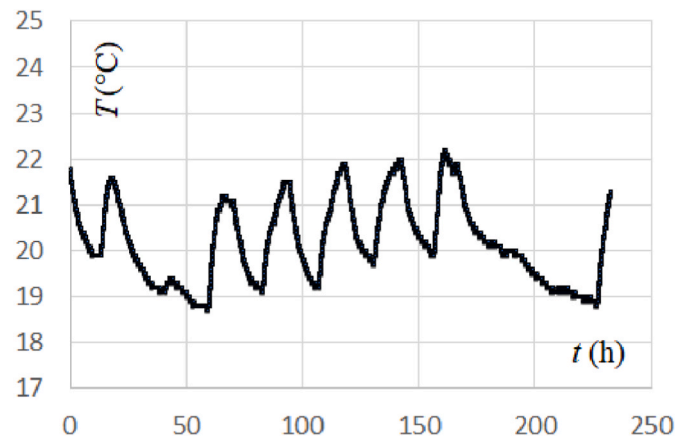
Fig. 6. Temperature fluctuations. Temperature fluctuations during 250 h of static long-term test.

explained by considering the adsorption of oxygen on the inner walls of the vacuum chamber. Through BLc, with a coating barrier, the gas flow is extremely low. Then, the rate of change for the O_2-coverage of surfaces in the chamber is expected to be slow. Saturation of the induced "capture pump" shows up after 250 *hours*. During this time there is a decrease of the effective pumping speed, while the oxygen flow continues to increase, then ending up with a noticeable change for the slope.

We observe that O_2-surface adsorption is not the only effect which can impact this analysis. Diffusion and adsorption are sensitive to the temperature changes. The temperature fluctuations in 250 h, measured by a thermistor close to the sample [10], are reported in Fig. 6.

The temperature gradient did not overcome 3 °C and the fluctuating behavior during night and day, allows to rule out that temperature variations can be the reason of a continuous increase in slope of $p_{d,SRG}$ in Fig. 5.

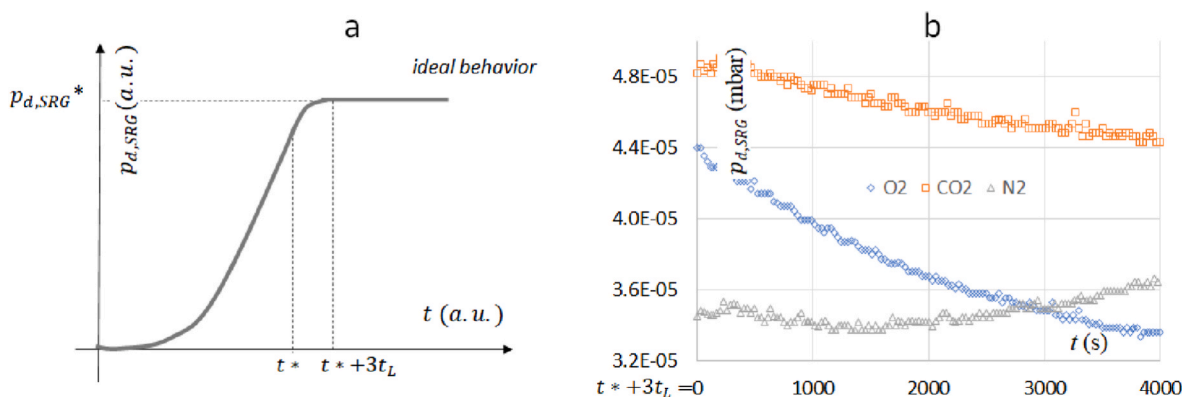However, if we can exclude the temperature fluctuations to be the

Fig. 7. Downstream pressure trend with no gas flow. (a) Ideal trend for downstream pressure $p_{d,SRG}$, which, after $t^* + 3t_L$, reaches a constant value $p_{d,SRG}$ * (neglecting vacuum chamber degas).(b) Real trend of $p_{d,SRG}$ for O_2, CO_2 and N_2 after $t^* + 3t_L$.

cause of the anomalous trend observed, we cannot do this for other phenomenon. For example, the time scale used for measurement can impact the quality of the polymer as it is experiencing a $10^5 Pa$ of O_2 differential pressure for multiple days. Then, to be able to distinguish between potential effects (e.g., accelerated aging [22]) impacting the trend seen in Fig. 5 for O_2 downstream pressure, we performed last tests changing the measurement procedure.

4.2.3. Static short-term test

For this third test, we keep on using the static method. To be able to exclude the effects of the potential aging of the polymer we use a completely different procedure. In this case BLc is exposed to $10^5 Pa$ of pure O_2 for a period of time (about one day) shorter than for the second test.

Here, at $t = 0\,s$ the upstream side of the sample is filled with tracer gas at $10^5 Pa$. Then, gas flow is stopped at a proper time t^* pumping the upstream side of the sample (bringing the upstream pressure p_u from $10^5 Pa$ to $1\,Pa$) and downstream pressure $p_{d,SRG}$ is monitored as reported in Fig. 7. For situation of negligible degas of the system, the pressure of tracer gas should remain constant after a short delay of $3t_L$, where t_L is diffusion lag time of the measurement as shown in Fig. 7 a.

This test is performed for a selection of three gases: O_2, CO_2, and N_2. Results are reported in Fig. 7 b setting the origin of the plot at $t^* + 3t_L$, to the time needed by the system to reach a steady state. The value t^* depends on the type of gas and is chosen in such a way to have the same tracer gas load quantity q inside the chamber before pumping the upstream side.

After 4000 s we observe a pressure drop of a 25% for O_2 and of an 8% for CO_2. On the contrary, we do not observe any analogous drop for N_2, whose pressure even starts to increase after 2000 s due to the expected chamber degassing. As the chamber volume is tested as leak-free and is isolated from the pumps, the only possible explanation for the pressure drop is gas adsorption on the surfaces of the inner walls. This phenomenon is clear for O_2 due to its considerable decrease in pressure and may also need to be considered for CO_2, which also shows a pressure drop. The trend of N_2, showing only after 2000 s the chamber degassing, does not completely exclude some partial N_2 adsorption on vacuum chamber. However, this phenomenon is negligible in comparison to the one seen for other tracer gases. Thus, also this third test is consistent with the hypothesis of potential O_2 adsorption on the inner walls of the chamber. The much shorter time extent of this latter experiment excludes that aging of the polymer can impact the results.

Thus, these three tests performed on BLc, make us confident in ascribing a relevant O_2 surface adsorption for a correct interpretation of measurement of the permeability coefficient of O_2 ultra-barrier materials. This appears true for both static and dynamic and for all ranges of time scales explored. Our study is going a step further than the one of ref. [11] performing also measurement without any ionization source and

thus it indicates a minor relevance for chemical reactions. We can conclude that O2 surface adsorption is one of the limiting factors for O_2 permeation measurements.

In future, we will focus on quantifying the oxygen adsorption, and would imagine a way to extend our set-up to WV permeability measurements in the challenging context of low reliability of a RGA detector [23].

5. General conclusions

This work demonstrates the extension of the applicability of the set-up firstly described in Ref. [10] to characterize films for food packaging applications. We have demonstrated the capability to measure permeabilities ranging from $10^{-8} cm^2/s$ to $10^{-11} cm^2/s$. A careful characterization of the apparatus has resulted in a minimum detectable gas throughput $2.5 \pm 0.5 \times 10^{-9} mbar\, l\, /\, s$. We were also able to show that oxygen adsorption inside the instrument is one of the artefacts to consider in the characterization of materials with low permeability. Across diverse sets of tests and methods of measurements, we could show that this effect is not negligible for our apparatus. The same effect is expected to occur when metallic manometric systems and optical–sensors-instrument built with metallic housing are employed.

CRediT authorship contribution statement

Marine Schott: Writing – review & editing, Writing – original draft, Data curation. **Janez Setina:** Supervision, Formal analysis, Data curation. **Espedito Vassallo:** Resources. **Matteo Pedroni:** Resources. **Roberta Campardelli:** Resources. **Patrizia Perego:** Resources. **Luca Repetto:** Writing – review & editing, Visualization, Formal analysis. **Giuseppe Firpo:** Writing – review & editing, Writing – original draft, Validation, Formal analysis, Data curation, Conceptualization.

Declaration of competing interest

The authors declare that they have no known competing financial interests or personal relationships that could have appeared to influence the work reported in this paper.

Data availability

The data that has been used is confidential.

References

[1] M. Zhang, X. Meng, B. Bhandari, Z. Fang, Crit. Rev. Food Sci. Nutr 56 (13) (2016) 2174–2182.

[2] Standard Test Method for Oxygen Gas Transmission Rate through Plastic Film and Sheeting Using Various Sensors, ASTM International Designation, 2008, 2622-08.

[3] K. Khanah Mokwena, J. Tang, Crit. Rev. Food Sci. Nutr. 52 (7) (2012) 640–650.

[4] M.G. Baschetti, M. Minelli, Polym. Test. 89 (2020), 106606.

[5] Standard Test Method for Oxygen Gas Transmission Rate through Plastic Film and Sheeting Using a Coulometric Sensor, ASTM International Designation, 2017. D3985-17.

[6] Standard Test Method for Determining Gas Permeability Characteristics of Plastic Film and Sheeting, ASTM International Designation, 2015, pp. D1434–D1482 (Reapproved.

[7] AMETEK, MOCON Inc.

[8] K. Muller, Z. Scheuerer, V. Florian, T. Skutschik, S. Sangerlaub, Polym. Test. 63 (2017) 126–132.

[9] X.D. Zhang, J.S. Lewis, C.B. Parker, J.T. Glass, S.D. Wolter, J. Vac. Sci. Technol., A 25 (6) (2007) 1587.

[10] G. Firpo, J. Setina, E. Angeli, L. Repetto, U. Valbusa, Vacuum 191 (2021), 110368.

[11] X.D. Zhang, J.S. Lewis, C.B. Parker, J.T. Glass, S.D. Wolter, J. Vac. Sci. Technol., A 26 (5) (2008) 1128.

[12] E. Vassallo, M. Aloisio, M. Pedroni, F. Ghezzi, P. Cerruti, R. Donnini, Coatings 12, 2022, p. 220.

[13] A.M. Horgan, I. Dalins, J. Vac. Sci. Technol. 10 (4) (1973) 559.

[14] Standard Test Method for Determining Gas Permeability Characteristics of Plastic Film and Sheeting, ASTM International Designation, 2015. D 1434-82 (Reapproved.

[15] J.G. Wijmans, R.W. Baker, J. Membr. Sci. 107 (1995) 1–21.

[16] J. Cranck, in: The Mathematics of Diffusions, second ed., Clarendon Press, Oxford, 1975, p. 51.

[17] M.V. Johansson, M. Wüest, P. Perrier, I. Graur, Phys. Fluids 34 (4) (2022), 046101.

[18] P. Pandey, R.S. Chauhan, Prog. Polym. Sci. 26 (2001) 853–893.

[19] L. Bao, J.R. Dorgan, D. Knauss, S. Hait, n.S. Oliveira, I.M. Maruccho, J. Membr. Sci. 285 (2006) 166–172.

[20] F. Welle, R. Franz, Polym. Test. 31 (2012) 93–101.

[21] D. Cava, E. Gimenez, R. Gavara, J.M. Lagaron, J. Plastic Film Sheeting 22 (4) (2006) 265–274.

[22] M. Frigione, A. Rodriguez-Prieto, Polymers 13 (2021) 2688.

[23] H. Yoshida, T. Ebina, K. Arai, T. Kobata, R. Ishii, T. Aizawa, A. Suzuki, Rev. Sci. Instrum. 88 (2017), 043301.